JOURNAL OF Materials CHEMISTRY

Static secondary ion mass spectrometry studies of self-assembled monolayers: electron beam degradation of alkanethiols on gold

David A. Hutt[a] **and Graham J. Leggett***[b]

[a]*Department of Materials Engineering and Materials Design, University of Nottingham, University Park, Nottingham, UK NG7 2RD*
[b]*Department of Chemistry, University of Manchester Institute of Science and Technology, PO Box 88, Manchester, UK M60 1QD*

Received 26th October 1998, Accepted 4th February 1999

Static secondary ion mass spectrometry (SIMS) has been used to investigate the degradation of self-assembled monolayers (SAMs) of alkanethiols subjected to bombardment by keV electrons. Because of its remarkable structural specificity, SIMS revealed significant structural modifications to the SAMs following irradiation. Both positive and negative ion spectra exhibited dramatic changes after exposure of SAMs to electron bombardment. In the positive ion spectra, peaks were observed between m/z 100 and 200 that were attributed to polycyclic aromatic ions with masses greater than the adsorbate molecule. These species are the result of interchain crosslinking initiated by electron impact. In the negative ion spectra, gold–molecular clusters disappeared after only small doses of electrons, attributed to the rapid oxidation of thiolates to disulfides. After doses as high as 3×10^{17} electrons cm^{-2}, there were still significant levels of sulfur at the surface along with graphitised carbonaceous material. It was concluded that keV electron impact leads to only slow removal of material from the SAM. These data illustrate the power of SIMS for probing surface reactions in SAMs.

Introduction

There has been considerable interest in the fabrication of patterned materials based on self-assembled monolayers (SAMs), and consequently much effort has been directed towards the development of techniques for the spatial control of SAM structure. On micron length scales, photolithography techniques have proved to be effective and convenient means by which patterned SAM structures may be fabricated,[1–4] and have been successfully employed in the control of cellular morphology.[5–7] Microcontact printing has also demonstrated efficacy at the micron scale,[8–11] and more recently, Whitesides and co-workers have provided elegant examples of sub-micron patterning using this approach.[12,13] However, the fabrication of structures on scales less than 100 nm presents considerable technical difficulties, and some workers have turned to electron beam techniques as an alternative approach. Using a focused electron beam, Lercel *et al.* created features as small as 25 nm in monolayers of *n*-octadecyltrichlorosilane (OTS) on SiO_2[14] and as small as 50 nm in monolayers of octadecanethiol (ODT) on GaAs.[14,15] They also employed STM lithography to pattern monolayers on GaAs, leading to the production of features as small as 15 nm.[16,17] More recently, they have demonstrated the feasibility of producing features smaller than 10 nm using electron beam techniques.[18] Carr *et al.* subsequently showed that nanostructures etched into SAMs on Si could be used to control the selective deposition of nickel using an electroless plating technique.[19] Sondag-Huethorst *et al.* used electron beam lithography to etch monolayers of docosanethiol on gold, and subsequently used the resulting nanostructures as positive resists for the galvanic deposition of copper,[20] and Schoer *et al.* have selectively deposited copper onto patterns created using STM.[21]

In the light of these impressive results, there has been interest in developing an understanding of the chemistry involved. Lercel *et al.* observed that the C1s signal did not decline to zero when they performed XPS on large areas of OTS monolayers following electron beam exposure.[17] Baer *et al.* also performed XPS on OTS SAMs that had been exposed to keV electrons, and observed little decline in the C1s signal.[22] However, they did report a small shift in the position of the C1s peak maximum, which they suggested was consistent with a graphitic structure following irradiation. A more detailed study was performed by Seshadri *et al.*, who used a variety of techniques including XPS, ellipsometry and IR spectroscopy[23] and arrived at similar conclusions. Gillen *et al.* used a microfocused electron beam to pattern SAMs of alkanethiols on Ag.[24] They reported that maximum replacement of the irradiated material by a fluorinated thiol was achieved after an electron dose of 2×10^{17} electrons cm^{-2}, but they estimated that the level of replacement was only of the order of 70%. They attributed this to the deposition of carbonaceous material at the surface following the interaction of energetic electrons with gaseous residual hydrocarbons in the vacuum system, which was only capable of achieving a vacuum of 7.5×10^{-4} Pa.

The only systematic studies of electron beam interactions with SAMs on gold are those of Olsen and Rowntree[25] and Volkel *et al.*[26] Olsen and Rowntree used vibrational spectroscopy to examine changes in the adsorbate alkyl chains. In agreement with the data from studies of silane SAMs, they concluded that C–H bond scission was caused by electronic interactions with SAMs, leading to crosslinking between alkyl chains. Volkel *et al.* studied changes in the carbon NEXAFS following exposure of SAMs of hexadecanethiol (HDT) to low energy electrons. They observed the growth of a sharp peak attributable to a C1s→π* transition, indicative of double bond formation.

While these studies provided important indications of the types of processes that occur following electron beam interactions with SAMs, data interpretation was not always straightforward. In particular, XPS peak shifts do not yield unambiguous chemical state assignments for complex organic materials, and infra-red techniques may not be sensitive to some of the changes that occur (for example, unsaturation[23]). We have been exploring the utility of secondary ion mass spectrometry (SIMS) for probing reactions within SAMs. In previous studies it has been shown that static SIMS is highly sensitive to changes in bonding within SAMs,[27,28] and recent research in the authors' laboratory has shown that SIMS may

be used highly effectively to study the kinetics of SAM photo-oxidation.[29,30] Despite this, however, SIMS has been relatively little used to study SAM reactivity. In the present study, SIMS has been employed to examine the changes in SAM structure that occur following electron bombardment. We have found that there are dramatic changes in the SIMS spectra of monolayers of octanethiol following keV electron bombardment, and that these changes may be readily interpreted to provide insights into the monolayer chemistry that confirm and augment the findings of earlier studies using other techniques.

Experimental

Preparation of monolayers

The SAMs were prepared on gold films supported on chromium-primed glass coverslips according to now standard procedures. The coverslips and glassware used in the sample preparation were first cleaned by soaking in hot 'Piranha' solution (a mixture of boiling hydrogen peroxide and sulfuric acid—CAUTION: Piranha solution is a strong oxidising agent) for 30 min, rinsed with copious amounts of distilled water and dried in an oven at 70 °C. Metal deposition was carried out by thermal evaporation from resistively heated Mo boats in a General Engineering bell jar vacuum system with a base pressure of $\sim 1 \times 10^{-6}$ Torr. A thin adhesive layer of chromium (99.99+%, Goodfellow Metals) was deposited first at a rate of 0.1 Å s^{-1} to a thickness of 30 Å. Gold was then deposited to a thickness of 300 Å at a rate of 0.5 Å s^{-1}. After allowing the substrates to cool, the bell jar was vented with N_2. The slides were removed from the evaporator and immediately immersed in 1 mM solutions of the octanethiol (OT, 96%, Fluka) in degassed ethanol (99.999% purity) for approximately 18 h. Following removal from the thiol solution, the substrates were rinsed with degassed ethanol and dried in a stream of nitrogen.

Secondary ion mass spectrometry

Secondary ion mass spectrometry (SIMS) was performed on a system equipped with a VG MM 12–12 quadrupole mass analyser and a VG liquid gallium metal ion gun (MIG). The primary ions were accelerated through a potential of 10 kV and focused into a spot less than 1 μm in diameter. The primary ion current used was *ca.* 0.8 nA. In spectroscopic mode, the beam was rastered at TV rate across a 25 mm^2 area, with the consequence that the current density at the sample surface was *ca.* 1.0 nA cm^{-2}. The primary dose was not allowed to exceed 5×10^{12} ions cm^{-2} in spectroscopic mode, in order to remain within the static regime, although higher doses were employed in imaging mode.

Electron bombardment

A beam of 4 keV electrons was generated using a VG LEG 63 electron gun. The beam was focused into a spot of approximately 50 μm diameter, and rastered across an area approximately 1 cm^2 in size. The dimensions and the position of the irradiated area were established using a copper grid sample, by detecting the secondary electron emission using a photomultiplier and forming an image. Using the ion-induced secondary electron image, the coordinates of the ion beam used to collect SIMS data were then set to fall within the irradiated area. The area from which data were collected by SIMS was smaller than the irradiated area, so that all of the SIMS data were collected from uniformly irradiated material. For each data point, a sample was exposed to the electron beam for the specified dose and positive and negative ion spectra were collected. Because exposure of the sample to gallium primary ions could lead to damage to the SAM, samples were discarded following a single SIMS analysis—the same sample was not repeatedly dosed and analysed. Consequently, in view of the minimisation of the dose during SIMS analysis, we can be confident that the changes

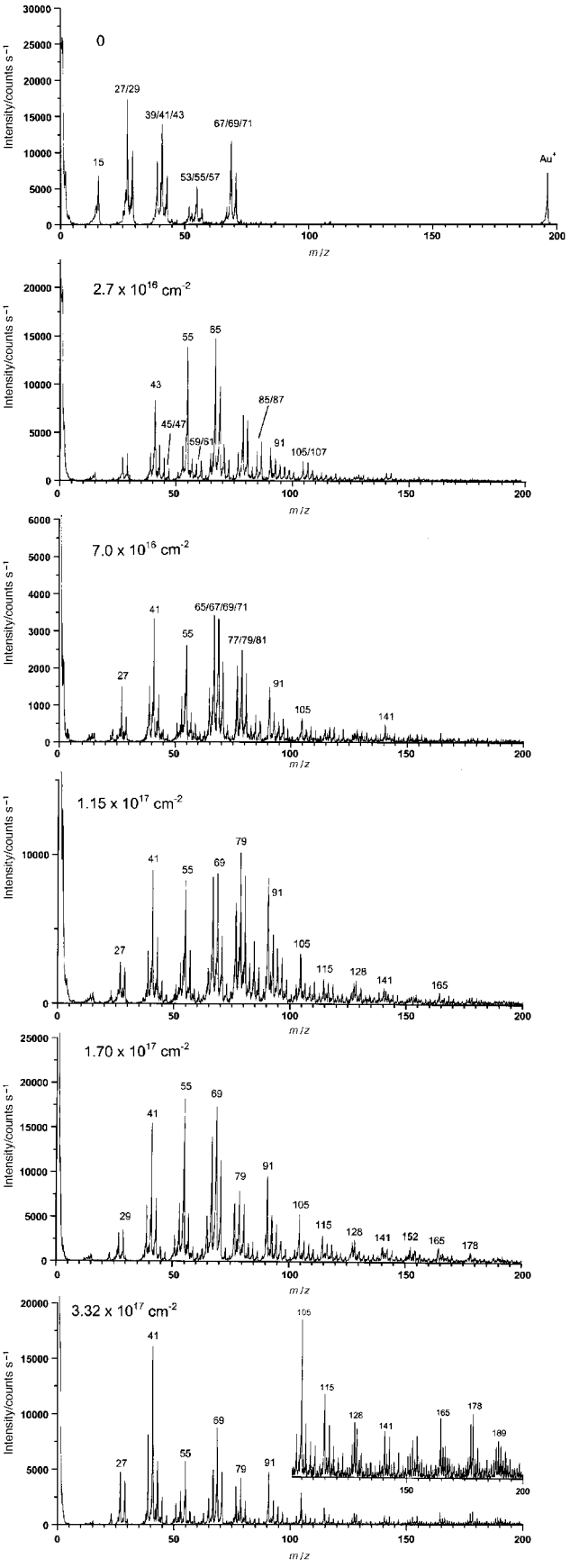

Fig. 1 Variation in the positive ion SIMS spectrum of octanethiol SAMs with exposure to 4 keV electrons.

observed in the SIMS spectra may be entirely attributed to electron-induced effects.

Results

Positive ion spectra

Fig. 1 shows positive ion SIMS spectra for OT SAMs subjected to increasing doses of electrons. The spectrum of the virgin material is relatively simple. There is a peak at m/z 197 corresponding to Au^+, and most of the other peaks may be interpreted by comparison with data obtained in previous detailed SIMS studies of hydrocarbon polymers.[31,32] Peaks at m/z 27/29, 39/41/43, 53/55/57 and 67/69/71 probably correspond to the hydrocarbon fragments $C_2H_3^+/C_2H_5^+$, $C_3H_3^+/C_3H_5^+/C_3H_7^+$, $C_4H_5^+/C_4H_7^+/C_4H_9^+$ and $C_5H_7^+/C_5H_9^+/C_5H_{11}^+$, respectively. There are no substantial peaks at higher m/z, however, and there is no molecular ion.

After a dose of only 2.7×10^{16} electrons cm^{-2}, the spectrum is significantly different. The Au^+ peak has been reduced to a negligible intensity. While the spectrum of the virgin material exhibits a small number of distinct clusters of peaks, the spectrum of the irradiated material is more complex, exhibiting more peaks and a less distinct separation into clusters. New peaks are evident at m/z 45/47 and 59/61. In previous studies, in which the spectra of SAMs and corresponding crystalline thiols were compared, peaks at m/z 47 and 61 were attributed to the ions $HS^+{=}CH_2$ and $HS^+{=}CHCH_3$, species that are generally characteristic of the mass spectra of thiols.[27,28] The peaks at m/z 47 and 61 in the spectra of irradiated OT SAMs possibly correspond to such species, with the peaks at m/z 45 and 59 representing reduced analogues; these ions are certainly not typical of hydrocarbon materials. Other new peaks are present at m/z 65 and 73 and 93–97 and are probably due to hydrocarbon ions. Peaks are also observed at m/z 105 and 107 that probably correspond to hydrocarbon ions ($C_8H_9^+$ and $C_9H_{11}^+$). However, peaks are also observed at m/z 85 and 87 that are not common hydrocarbon species, and are not observed in the spectra of either undamaged OT SAMs or polyethylene. An unequivocal assignment of these peaks is not possible, but most likely, they are sulfur-containing species ($C_4H_5S^+$ and $C_4H_7S^+$ respectively). Finally, a peak is also clearly evident at m/z 91, probably corresponding to the tropylium ion, $C_7H_7^+$.

After 7×10^{16} electrons cm^{-2}, these changes are again clearly evident, and the intensity of the peak due to the tropylium ion is increased in intensity. The tropylium ion continues to increase in intensity with increasing electron dose, and by 1.15×10^{17} electrons cm^{-2}, it is nearly the most intense peak in the spectrum. The peak at m/z 85 remains significant, and new peaks begin to appear (albeit weakly) above m/z 100, including m/z 115, 128/9, 141 and 165. The peak at m/z 105 remains prominent.

After a dose of 1.7×10^{17} electrons cm^{-2}, the peaks above m/z 100 are clearly evident, and they become increasingly distinct with increasing exposure until, after 3.3×10^{17} electrons cm^{-2}, the region between m/z 100 and 200 exhibits prominent peaks at m/z 105, 115, 128/9, 141, 165, 178/9 and 189. Peaks at these m/z values have been observed in the SIMS spectra of polystyrene (PS)[33] and ion-beam damaged polymers,[34,35] and have been attributed to polycyclic aromatic ions.

Negative ions

The negative ion spectra of freshly prepared SAMs contain a number of gold–molecular fragments, including the species $Au(M-H)^-$, $Au(M-H)S^-$ and $Au(M-H)_2^-$, where M is the adsorbate molecule (Fig. 2). These species were observed in the negative ion SIMS spectrum of OT in the present study. Peaks were also observed due to the ions Au^-, AuS^-, Au_2^- and Au_2S^-, and these are again typical of the negative ion SIMS spectra of freshly prepared SAMs.[28] At low m/z, peaks were also observed that are due to CH^- (m/z 13), C_2H^- (m/z 25), S^- and SH^- (m/z 32 and 33 respectively).

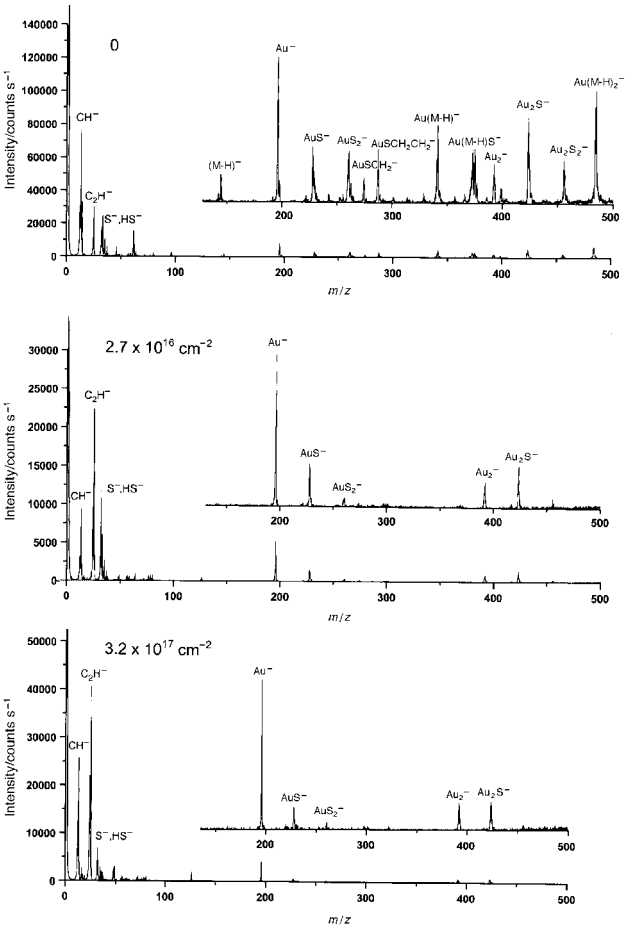

Fig. 2 Variation in the negative ion SIMS spectrum of octanethiol SAMs with exposure to 4 keV electrons.

After only small exposures to electrons, the molecular species were completely lost from the negative ion spectra. Fig. 2 shows a spectrum recorded after exposure to 2.7×10^{16} electrons cm^{-2}. The peak at m/z 13, due to CH^-, was much reduced in intensity, while the peak at m/z 25, due to C_2H^-, was significantly larger relative to the S^- peak. However, the peaks due to Au^- and AuS^- remained, and continued to remain even after very large doses of electrons. Few qualitative changes were observed in the negative ion spectra on increasing the dose to 3.2×10^{17} electrons cm^{-2}, and the Au^- and AuS^- peaks both remained clearly evident. In order to determine whether there were any quantitative changes in the spectra, the relative intensity ratios were calculated for some key ions in the negative ion spectra. Desorption of sulfur should lead to a relative reduction in the magnitude of the AuS^- peak relative to the Au^- peak, and in the intensity of the sulfur peaks S^- and SH^- relative to the nearby carbon fragment, C_2H^-, so the ratios shown in expressions (1) and (2) were calculated.

$$Y_1=[AuS^-]/\{[AuS^-]+[Au^-]\} \quad (1)$$

$$Y_2=[S^-+HS^-]/\{[S^-+HS^-]+[C_2H^-] \quad (2)$$

Here [X] is the peak area of species X in the SIMS spectrum. These ratios are plotted against the dose of electrons in Fig. 3. There is an initial sharp drop in Y_2, reflecting the sudden rise in the intensity of C_2H^-, but thereafter, both ratios change in a similar fashion with dose, and neither changes very significantly. As the dose increases from 2.5×10^{16} to 3.2×10^{17} electrons cm^{-2}, Y_1 falls by about one third, while Y_2 falls by

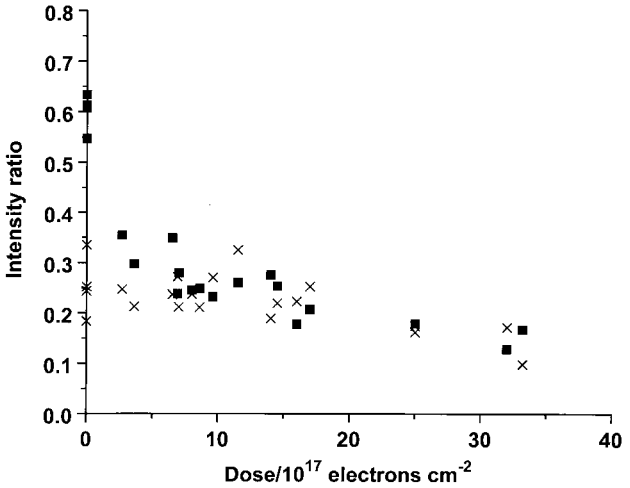

Fig. 3 Variation in the relative intensity ratios $Y_1=[AuS^-]/\{[AuS^-]+[Au^-]\}$ (crosses) and $Y_2=[S^-+HS^-]/\{[S^-+HS^-]+[C_2H^-]\}$ (squares) with exposure to 4 keV electrons.

Table 1 Structures of polycyclic aromatic ions

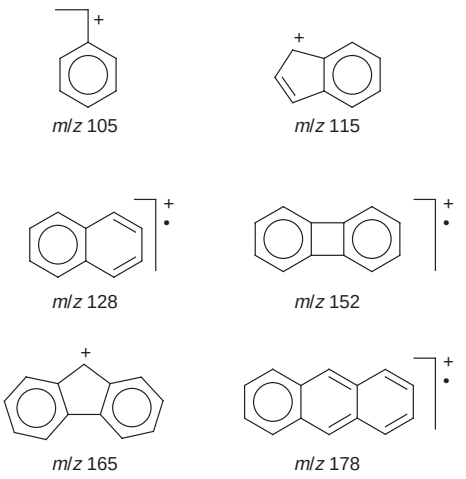

about one half. This implies that over this period, there is a small reduction in the sulfur content of the surface, but that significant quantities of sulfur remain even after very large exposures to electrons.

Discussion

Positive ion spectra

The changes to the positive ion spectra of OT monolayers following exposure to keV electrons are substantial and provide important insights into the nature of the changes induced in the SAM structure. The observation of increased yields of high molecular weight hydrocarbon ions following only short exposures to electrons is indicative of significant changes in ion formation probabilities as a result of electron–SAM interactions. The positive ion spectra of fresh SAMs exhibit few large hydrocarbon ions,[27–30] in contrast to the spectra of hydrocarbon polymers such as polyethylene.[31] This difference is because of the dominant role of the sulfur–metal interaction in determining the outcome of SAM fragmentation,[27,28] and the observation of significant numbers of large hydrocarbon ions following exposure to small doses of electrons indicates that there are rapid changes to the sulfur bonding environment. Further support for this hypothesis comes from the decline in the Au^+ intensity. The yield of Au^+ from clean gold films is small,[28] and its increase in the spectra of fresh SAMs may be attributed to the electronegative sulfur, thought to be present as a thiolate. The decline in the Au^+ intensity is best explained by a change in the Au–S interaction. One possibility is that electron exposure of the SAMs leads to oxidation of thiolates to disulfides, with an accompanying reduction of gold surface atoms.

In earlier studies, positive ion SIMS spectra of crystalline thiols were found to be dominated by ions containing sulfur as the primary charge-site,[27,28] whereas positive ion spectra of corresponding SAMs were found to contain only small alkyl chain fragments that did not contain S.[24,25,28] If we are correct in attributing peaks at *m/z* 47, 61 and 85/7 to sulfur-containing species, similar to those formed from thiol compounds in electron impact mass spectrometry, then it may be inferred that electron impact with SAMs leads to scission of the S–Au bond, in agreement with the discussion in the preceding paragraph.

The appearance of a tropylium ion at *m/z* 91, an ion associated with the spectra of aromatic polymers and organic molecules, is indicative of extensive conjugation, consistent with the elimination of hydrogen and the formation of multiple double bonds in the adsorbates. The peaks that appear between *m/z* 100 and 200 in the electron-irradiated material also provide evidence that hydrogen elimination is occurring. In the SIMS spectrum of polystyrene, a range of peaks are observed in this mass range that have polycyclic aromatic structures (see Table 1)[33] and that correspond to the peaks observed in the electron beam damaged SAMs. One exception occurs at *m/z* 105; this ion is weak in the spectrum of PS, which instead has a stronger peak at *m/z* 103. However, in plasma-polymerised styrene, the *m/z* 105 peak predominates, and is associated with cross-linking.[36] These ions are also observed in the SIMS spectra of ion-beam damaged poly(vinyl chloride) (PVC) and poly(methyl methacrylate) (PMMA)[34,35] (although again, *m/z* 105 is larger than *m/z* 103). Ion-beam degradation of these materials, like gamma- and electron-induced degradation, is thought to result in the elimination of pendant groups and the formation of polyene structures, with the result that formation of highly unsaturated ion structures during SIMS becomes much easier. Polycyclic aromatic ions are highly stable structures, and the cyclisation of long chain fragments is thought to be relatively facile.[33,37] Indeed, because of the ease with which HCl is eliminated from PVC, polycyclic aromatic ions are observed with reasonable intensity in SIMS spectra of the undamaged material.[34] The observation of these types of ions in the SIMS spectra of electron beam damaged SAMs thus provides good evidence that hydrogen elimination is occurring.

Above *m/z* 105, these polycyclic aromatic ions contain more carbon atoms than the intact adsorbate molecule. The anthracene ion ($C_{14}H_{10}^+$, *m/z* 178) exhibits a significant intensity, and ions containing as many as 16 carbon atoms were observed. The observation of such large ions provides clear evidence that cross-linking between the adsorbate alkyl chains results from electron irradiation of SAMs. In contrast to the changes that occur in S–Au bonding, however, cross-linking occurs over a longer time period, and the polycyclic aromatic ions are observed to increase slowly with increasing electron exposure up to 3×10^{17} electrons cm^{-2}. Taken together, the evidence for the presence of cross-linked and unsaturated material in the SAM following irradiation provides strong evidence for the formation of a graphitic layer. This is in agreement with the suggestions made by other workers that graphitic material is formed following irradiation of SAMs formed on other substrates.[17,22,23] However, in contrast to the XPS data presented in these studies, which relied upon compositional data[17,22,23] and a rather small shift in the position of the C1s peak,[22,23] the SIMS data are much clearer and provide much less ambiguous indications of the nature of the damaged material.

The clear evidence provided for cross-linking here is in sharp contrast to the data obtained in previous SIMS studies of photooxidation of SAMs on Ag[29] and Au.[30] In those studies, we observed no polycyclic aromatic ions, and the positive ion SIMS spectra exhibited few large ions. We thus conclude that cross-linking does not occur during SAM photooxidation, even after long exposures (for example, complete oxidation of a SAM of 11-mercaptoundecanoic acid did not occur until the sample had been exposed to a medium pressure mercury arc lamp for five hours[30]). In a recent study, Schoenfisch and Pemberton claimed to have observed bands at 1390 and 1590 cm^{-1} in the Raman spectra of oxidised SAMs on Au, which they attributed to graphitised material.[38] This is quite at odds with our findings; if the data reported by Schoenfisch and Pemberton are correct, they are more consistent with the behaviour reported in the present study for electron bombardment of SAMs than with that reported earlier for photooxidised SAMs.

Negative ions

The rapid and complete disappearance of gold–molecular species such as $Au(M-H)^-$ from the negative ion spectra is indicative of a change in the nature of the gold–adsorbate interaction. While alkyl chain fragmentation alone might be expected to lead to a change in the composition of the gold–molecular fragments in the spectrum, it would not be expected to lead to a complete loss of such species, but, rather, the appearance of smaller fragments (*e.g.* $Au(M-H-nCH_2)^-$). The rapidity of this change is indicative of a facile chemical transformation of the Au–S environment. Given that the amount of sulfur in the samples declined only slowly with dose, and the persistence of high m/z hydrocarbon ions in the positive ion spectra, this change in the Au–S environment must be much more rapid than any other process that results from electron impact with the SAMs. The rapid disappearance of the Au^+ species from the positive ion spectra is not mirrored by a disappearance of the S^- and HS^- species; while the relative intensities of these peaks drop relative to the C_2H^- ion, they remain approximately constant relative to the Au^- ion. Similarly, the intensity of the AuS^- species changes only slowly relative to the Au^- intensity. The implication of this is that change in the Au–S bonding environment occurs without significant loss of sulfur from the surface. The appearance of ions in the positive ion spectrum that are probably due to sulfur–carbon fragments suggests that cleavage of the S–C bond does not accompany cleavage of S–Au bonds.

The conclusion that seems most likely based on these data is that the thiolates are rapidly oxidised to disulfides on exposure to electrons, with the concomitant result that gold surface sites are reduced to Au^0. This conclusion is very much in line with the work of Jager *et al.*,[39] who observed two oxidation states for S following X-ray induced damage to SAMs of alkanethiols on Au. They attributed this to thiol oxidation induced by low energy secondary electrons. Wirde *et al.* also reported that ionising radiation caused scission of S–Au bonds in SAMs, leading to the formation of disulfides.[40] In a quite different context, Riederer *et al.* reported the ready cleavage of S–Au bonds in low energy processes induced by keV ion bombardment.[41] While they speculated that combination of thiolates with hydrogen may occur, disulfide formation is also possible.

General remarks

XPS has proved to be a very valuable tool for the characterisation of SAMs. Of particular importance is its ability to provide quantitative compositional data relatively straightforwardly. XPS also yields chemical structural information. However, the magnitudes of the chemical shifts observed for carbon may be small, and are often ambiguous. Electron-beam degradation provides an illustration of the complexities of XPS analysis. While a shift in the C1s peak position does occur, it is small and far from unambiguous. In contrast, static SIMS has revealed marked changes in the surface structure, through the observation of a range of high m/z unsaturated and aromatic species. While IR spectroscopy has also been a powerful probe for SAM structure, it yields limited information on the S–Au interaction and is not well suited to following the development of unsaturation in SAMs.[23] Similarly, while XPS does yield information on the S bonding environment, the S2p peak is typically small and noisy, and peak fitting is thus difficult and subject to uncertainty. In contrast, clear and dramatic changes are observed in the negative ion SIMS spectra as a result of electron beam degradation of SAMs. These changes provide a straightforward means to evaluate changes in the S–Au bond, and indicate that SIMS may have an important role to play in fundamental studies of thiol–gold interactions. While SIMS undoubtedly has difficulties of its own, not least the complexities of spectral interpretation, the data that it can provide are powerful and often unavailable through the application of other techniques. Recent studies have provided evidence that careful, detailed systematic work on SAM reactivity is possible using SIMS;[29,30,42] the present data add strength to the argument that SIMS is a powerful probe for SAM structure and reactivity.

Conclusions

Static SIMS spectra exhibit marked changes on exposure of monolayers of octanethiol to keV electrons. The positive spectra exhibit a range of peaks between m/z 100 and 200 that are due to polycyclic aromatic ions and that are indicative of the formation of an unsaturated, cross-linked structure. The negative ion spectra exhibit a sudden and complete loss of gold–molecular species following exposure to only small doses of electrons, that is indicative of electron-induced oxidation of thiolates to disulfides, accompanied by reduction of gold surface sites. The amount of sulfur in the SAM declines only slowly, indicating that electron bombardment leads to a slow removal of adsorbate material. Static SIMS has been shown to be a powerful and sensitive probe for changes in SAM structure and bonding.

Acknowledgements

The authors are grateful to the EPSRC (grant GR/K28671) for financial support. GJL wishes to thank the Nuffield Foundation for a Science Research Fellowship.

References

1 M. J. Tarlov, D. R. F. Burgess and G. Gillen, *J. Am. Chem. Soc.*, 1993, **115**, 5305.
2 G. Gillen, J. Bennett, M. J. Tarlov and D. R. F. Burgess, *Anal. Chem.*, 1994, **66**, 2170.
3 J. Huang and J. C. Hemminger, *J. Am. Chem. Soc.*, 1993, **115**, 3342.
4 J. Huang, D. A. Dahlgren and J. C. Hemminger, *Langmuir*, 1994, **10**, 626.
5 D. A. Hutt, E. Cooper, L. Parker, G. J. Leggett and T. L. Parker, *Langmuir*, 1996, **12**, 5494.
6 E. Cooper, R. Wiggs, D. A. Hutt, L. Parker, G. J. Leggett and T. L. Parker, *J. Mater. Chem.*, 1997, **7**, 435.
7 C. A. Scotchford, E. Cooper, G. J. Leggett and S. Downes, *J. Biomed. Mater. Res.*, 1998, **41**, 431.
8 A. Kumar, H. A. Biebuyck and G. M. Whitesides, *Langmuir*, 1994, **10**, 1498.
9 Y. Xia, E. Kim and G. M. Whitesides, *J. Electrochem. Soc.*, 1996, **143**, 1070.
10 M. Mrksich, C. S. Chen, Y. Xia, L. E. Dike, D. E. Ingber and G. M. Whitesides, *Proc. Natl. Acad. Sci. USA*, 1996, **93**, 10775.

11 Y. Xia, J. Tien, D. Qin and G. M. Whitesides, *Langmuir*, 1996, **12**, 4033.
12 Y. Xia and G. M. Whitesides, *Langmuir*, 1997, **13**, 2059.
13 Y. Xia and G. M. Whitesides, *Angew. Chem.*, *Int. Ed.*, 1998, **37**, 550.
14 M. J. Lercel, R. C. Tiberio, P. F. Chapman, H. G. Craighead, C. W. Sheen, A. N. Parikh and D. L. Allara, *J. Vac. Sci. Technol. B*, 1993, **11**, 2823.
15 R. C. Tiberio, H. G. Craighead, M. Lercel, T. Lau, C. W. Sheen and D. L. Allara, *Appl. Phys. Lett.*, 1993, **62**, 476.
16 M. J. Lercel, G. F. Redinbo, F. D. Pardo, M. Rooks, R. C. Tiberio, P. Simpson, H. G. Craighead, C. W. Sheen, A. N. Parikh and D. L. Allara, *J. Vac. Sci. Technol. B*, 1994, **12**, 3663.
17 M. J. Lercel, M. Rooks, R. C. Tiberio, H. G. Craighead, C. W. Sheen, A. N. Parikh and D. L. Allara, *J. Vac. Sci. Technol. B*, 1995, **13**, 1139.
18 M. J. Lercel, H. G. Craighead, A. N. Parikh, K. Seshadri and D. L. Allara, *Appl. Phys. Lett.*, 1996, **68**, 1504.
19 D. W. Carr, M. J. Lercel, C. S. Whelan, H. G. Craighead, K. Seshadri and D. L. Allara, *J. Vac. Sci. Technol. A*, 1997, **15**, 1446.
20 J. A. M. Sondag-Huethorst, H. R. J. van Helleputte and L. G. J. Fokkink, *Appl. Phys. Lett.*, 1994, **64**, 285.
21 J. K. Schoer, C. B. Ross, R. M. Crooks, T. S. Corbitt and M. Hampden-Smith, *Langmuir*, 1994, **10**, 615.
22 D. R. Baer, M. H. Engelhard, D. W. Schulte, D. E. Guenther, L.-Q. Wang and P. C. Rieke, *J. Vac. Sci. Technol. A*, 1994, **12**, 2478.
23 K. Seshadri, K. Froyd, A. N. Parikh, D. L. Allara, M. J. Lercel and H. G. Craighead, *J. Phys. Chem.*, 1996, **100**, 15900.
24 G. Gillen, S. Wight, J. Bennett and M. J. Tarlov, *Appl. Phys. Lett.*, 1994, **65**, 534.
25 C. Olsen and P. A. Rowntree, *J. Chem. Phys.*, 1998, **108**, 3650.
26 B. Volkel, A. Golzhauser, H. U. Millar, C. David and M. Grunze, *J. Vac. Sci. Technol. B*, 1997, **15**, 2877.
27 G. J. Leggett, M. C. Davies, D. E. Jackson and S. J. B. Tendler, *J. Chem. Soc.*, *Faraday Trans.*, 1993, **89**, 179.
28 G. J. Leggett, M. C. Davies, D. E. Jackson and S. J. B. Tendler, *J. Phys. Chem.*, 1993, **97**, 5348.
29 D. A. Hutt, E. Cooper and G. J. Leggett, *J. Phys. Chem. B*, 1998, **102**, 174.
30 E. Cooper and G. J. Leggett, *Langmuir*, 1998, **14**, 4795.
31 G. J. Leggett, D. Briggs and J. C. Vickerman, *Surf. Interface Anal.*, 1991, **17**, 737.
32 D. Briggs, *Surf. Interface Anal.*, 1990, **15**, 734.
33 G. J. Leggett, J. C. Vickerman, D. Briggs and M. J. Hearn, *J. Chem. Soc.*, *Faraday Trans.*, 1992, **88**, 297.
34 G. J. Leggett and J. C. Vickerman, *Appl. Surf. Sci.*, 1992, **55**, 105.
35 D. Briggs and M. J. Hearn, *Vacuum*, 1986, **36**, 1005.
36 G. J. Leggett, B. D. Ratner and J. C. Vickerman, *Surf. Interface Anal.*, 1995, **23**, 22.
37 G. J. Leggett and J. C. Vickerman, *Int. J. Mass Spectrom. Ion Processes*, 1992, **122**, 281.
38 M. H. Schoenfisch and J. E. Pemberton, *J. Am. Chem. Soc.*, 1998, **120**, 4502.
39 B. Jager, H. Schurmann, H. U. Muller, H. J. Himmel, M. Neumann, M. Grunze and C. Woll, *Phys. Chem.*, 1997, **202**, 263.
40 M. Wirde, U. Gelius, T. Dunbar and D. L. Allara, *Nucl. Instrum. Methods Phys. Res.*, *Sect. B*, 1997, **131**, 245.
41 D. E. Riederer, R. Chatterjee, S. W. Rosencrance, Z. Postawa, T. D. Dunbar, D. L. Allara and N. Winograd, *J. Am. Chem. Soc.*, 1997, **119**, 8089.
42 S. Pan, D. G. Castner and B. D. Ratner, *Langmuir*, 1998, **14**, 3545.

Paper 8/08257J